Supplementary Figure 1

a

	eQTL	sQTL	ieQTL	isQTL

No
Yes
NaN

b

GTEx

Total=279

NaN (n = 1)
None (n = 4)
eQTL (n = 60)
eQTL, ieQTL (n = 10)
eQTL, sQTL (n = 144)
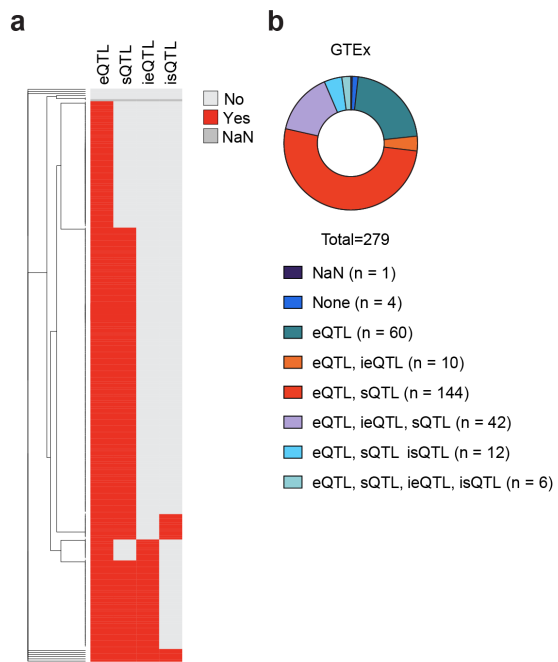eQTL, ieQTL, sQTL (n = 42)
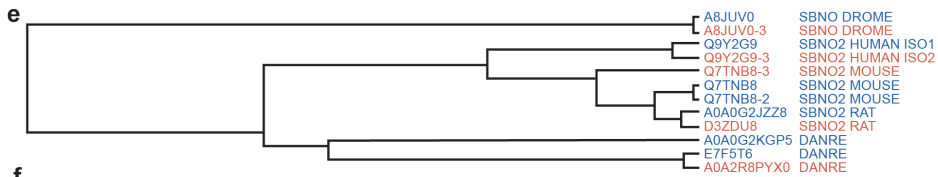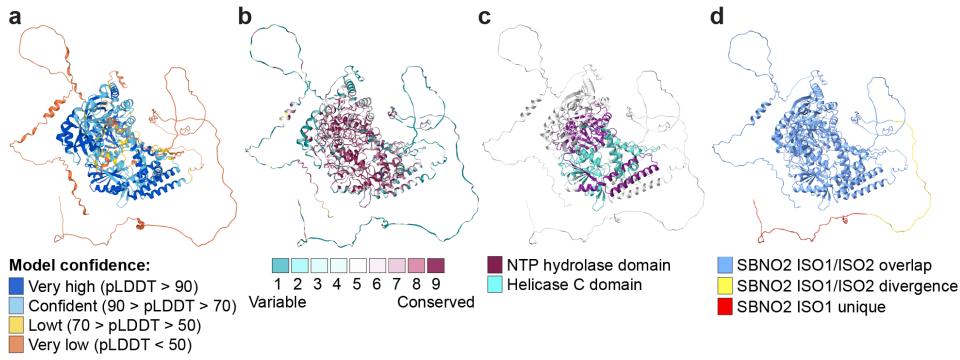eQTL, sQTL isQTL (n = 12)
eQTL, sQTL, ieQTL, isQTL (n = 6)

Supplementary Figure 1: GTEx eQTL, sQTL, ieQTL, and isQTL analysis of confident GWAS IBD genes. (a) Heatmap presentation of the presence or absence of GTEx eQTL, sQTL, ieQTL, and isoQTL across confident GWAS IBD genes[2] (n = 279, Bolton C. et al., Gastroenterology 2022, Supplementary Table 4: Genes included in the analysis of the intersection of monogenic IBD genes and polygenic IBD loci). (b) Pie chart presentation of numbers of confident GWAS IBD genes according to (a). Source data are provided as a Source Data file for Supplementary Figure 1a.

Supplementary Figure 2

Chromosome 19 Coordinate (Mb) (GRCh37)
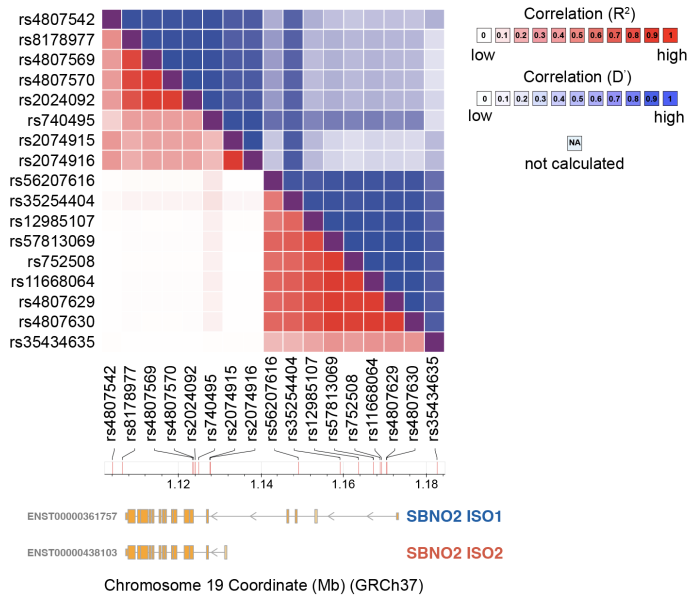
Supplementary Figure 2: LDlink linkage disequilibrium analysis of variants in *SBNO2* with GWAS-based association with IBD/CD.
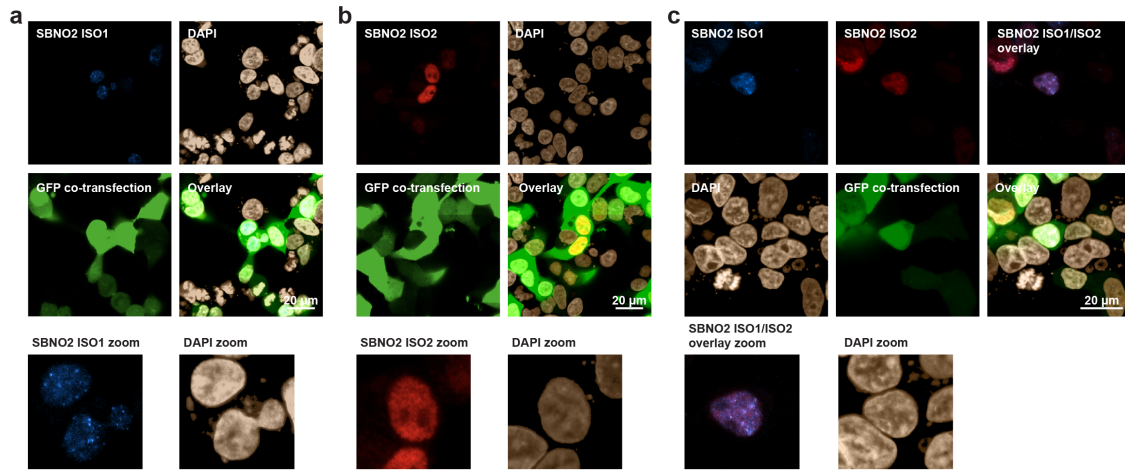
Supplementary Figure 3

a

b

c

d

Model confidence:
- Very high (pLDDT > 90)
- Confident (90 > pLDDT > 70)
- Lowt (70 > pLDDT > 50)
- Very low (pLDDT < 50)

1 2 3 4 5 6 7 8 9
Variable   Conserved

- NTP hydrolase domain
- Helicase C domain

- SBNO2 ISO1/ISO2 overlap
- SBNO2 ISO1/ISO2 divergence
- SBNO2 ISO1 unique

e

A8JUV0	SBNO DROME	
A8JUV0-3	SBNO DROME	
Q9Y2G9	SBNO2 HUMAN ISO1	
Q9Y2G9-3	SBNO2 HUMAN ISO2	
Q7TNB8-3	SBNO2 MOUSE	
Q7TNB8	SBNO2 MOUSE	
Q7TNB8-2	SBNO2 MOUSE	
A0A0G2JZZ8	SBNO2 RAT	
D3ZDU8	SBNO2 RAT	
A0A0G2KGP5	DANRE	
E7F5T6	DANRE	
A0A2R8PYX0	DANRE	

f

Q7TNB8	SBNO2 MOUSE	1	--MLAVEPTMDGDFPPHEL-PPP	20
Q7TNB8-2	SBNO2 MOUSE	1	--MLAVEPTMDGDFPPHEL-PPP	20
Q7TNB8-3	SBNO2 MOUSE	1	--	0
Q9Y2G9	SBNO2 HUMAN ISO1	1	--MLAVGPAMDRDYPQHEP-PPA	20
Q9Y2G9-3	SBNO2 HUMAN ISO2	1	--	0
A0A0G2JZZ8	SBNO2 RAT	1	---MPTLATSVVMDTEDYLHPEGPQL	23
D3ZDU8	SBNO2 RAT	1	--MLAVEPTMDGDFPPHEL-PPP	20
E7F5T6	DANRE	1	--	0
A0A0G2KGP5	DANRE	1	---MPSLSIPPAMDGHSFSNSVGPQL	23
A0A2R8PYX0	DANRE	1	--	0
A8JUV0	SBNO DROME	181	KLNNMVTAMGSPAARSSGNAGTTGSSQGGAIGSTSSYLNSLTTNELMNLAAYVAA-----	235
A8JUV0-3	SBNO DROME	181	KLNNMVT---	187

Q7TNB8	SBNO2 MOUSE	21	GG--GI----QLQNRLL----HCPWWGSFSPSL----YPTFSSENQQFVGSTPFLGGQSC	66
Q7TNB8-2	SBNO2 MOUSE	21	GG--GI----QLQNRLL----HCPWWGSFSPSL----YPTFSSENQQFVGSTPFLGGQSC	66
Q7TNB8-3	SBNO2 MOUSE	1	--	0
Q9Y2G9	SBNO2 HUMAN ISO1	21	GS--LLYSPPPLQSAML----HCPYWNTFSLPP----YPAFSSDSRPFMSSASFLGSQPC	70
Q9Y2G9-3	SBNO2 HUMAN ISO2	1	-------------------------------MREPLPGSASWGTPGPP	17
A0A0G2JZZ8	SBNO2 RAT	24	GSPKFSAPSPPLTSSMESQLYQPNSWAYSQQAQYNQHYPMQSGRQLQ-----------	70
D3ZDU8	SBNO2 RAT	21	GG--GI----QLQNRLL----HCPWWGSFSPPL----YPTFSSENQQFVSSTPFLGGQSC	66
E7F5T6	DANRE	1	--MALLGDQN-	8
A0A0G2KGP5	DANRE	24	DARGFVLATP------MSHVFANNHWSFPNQP-FGLPCPAQSENQQS------CFNGVSD	70
A0A2R8PYX0	DANRE	1	--	0
A8JUV0	SBNO DROME	236	--KGSNAPPPPPPSTAANSVRHSPTGGIPN--------P-----------GGNFFGGSAA	274
A8JUV0-3	SBNO DROME	188	--	187

Q7TNB8	SBNO2 MOUSE	67	PETSYPTTATV---PSFFSKSSDFPQDPSCLEDLSNASV--FSSSVDSLSDIPDTPD---	118
Q7TNB8-2	SBNO2 MOUSE	67	PETSYPTTATV---PSFFSKSSDFPQDPSCLEDLSNASV--FSSSVDSLSDIPDTPD---	118
Q7TNB8-3	SBNO2 MOUSE	1	---------MSQ---LRFWLQFEALNKDPSCLEDLSNASV--FSSSVDSLSDIPDTPD---	44
Q9Y2G9	SBNO2 HUMAN ISO1	71	PDTSYAPVATA---SSLPPKTCDFAQDSSYFEDFSNISI--FSSSVDSLSDIVDTPD---	122
Q9Y2G9-3	SBNO2 HUMAN ISO2	18	----SAGTMSQ---LQLWLQFEALNKDSSYFEDFSNISI--FSSSVDSLSDIVDTPD---	65
A0A0G2JZZ8	SBNO2 RAT	71	PTPSFMNLDLSDIDFHELVRNGDFSQELPCTDEV--ASL--FSSPSDSLLEYPEP-S---	122
D3ZDU8	SBNO2 RAT	67	PETSYPTTATV---PSFFSKSSDFPQDPSCLEDLSNASV--FSSSVDSLSDIPDTPD---	118
E7F5T6	DANRE	9	---SFTVPCGI---------PTLGVQDPSCLEDLSNASV--FSSSVDSLSDIPDTPD---	51
A0A0G2KGP5	DANRE	71	MHTDLLPQDLSNFDFSGL----DLPQDLSCLDDQ---LI--FSPQNDSLSEYAST-N---	117
A0A2R8PYX0	DANRE	1	--MSLMQIWTKLYAQLGR----PPPKDLSCLDDQ---LI--FSPQNDSLSEYAST-N---	45
A8JUV0	SBNO DROME	275	ASTSASAAN-FNMAASLL-------AQMSYAGGASQIRALKVAGNIGCVGNNQKPPPIAT	326
A8JUV0-3	SBNO DROME	188	--------------------------VSYAGGASQIRALKVAGNIGCVGNNQKPPPIAT	220

Q7TNB8	SBNO2 MOUSE	119	---------FLQADSL-------NEVPTIWDV------STTSTTHDKLFIPSGPFSAP--	154
Q7TNB8-2	SBNO2 MOUSE	119	---------FLQADSL-------NEVPTIWDV------STTSTTHDKLFIPSGPFSAP--	154
Q7TNB8-3	SBNO2 MOUSE	45	---------FLQADSL-------NEVPTIWDV------STTSTTHDKLFIPSGPFSAP--	80
Q9Y2G9	SBNO2 HUMAN ISO1	123	---------FLPADSL-------NQVSTIWDD------NPAPSTHDKLFQLSRPFAGF--	158
Q9Y2G9-3	SBNO2 HUMAN ISO2	66	---------FLPADSL-------NQVSTIWDD------NPAPSTHDKLFQLSRPFAGF--	101
A0A0G2JZZ8	SBNO2 RAT	123	---------GFGTDSLAQLTGEGPAAQMYWDI------PGHSQRPLN----LSAFPG---	160
D3ZDU8	SBNO2 RAT	119	---------FLPADSL-------NEVPTIWDV------STTSTTRDKLFPSVPFSAL--	154
E7F5T6	DANRE	52	---------FLPADSL-------NEVPTIWDV------STTSTTRDKLFLPSVPFSAL--	87
A0A0G2KGP5	DANRE	118	---------FLNA-------DMAPTVPTIWDI------KTPAPVQES----SNRFQGLN-	150
A0A2R8PYX0	DANRE	46	---------FLNA-------DMAPTVPTIWDI------KTPAPVQES----SNRFQGLN-	78
A8JUV0	SBNO DROME	327	TPGSGGPAGGAPGSGVKGNNSMMEAVQKLIAMNPEYLTSGIPNTVFQMFMQSMQRPQATP	386
A8JUV0-3	SBNO DROME	221	TPGSGGPAGGAPGSGVKGNNSMMEAVQKLIAMNPEYLTSGIPNTVFQMFMQSMQRPQATP	280

Q7TNB8	SBNO2 MOUSE	155	--EDPV--TSLSSTPLLISYQ-SH---SQPEEEEGEEEEETEELGHAETYADYVPSKSKI	206
Q7TNB8-2	SBNO2 MOUSE	155	--EDPV--TSLSSTPLLISYQ-SH---SQPEEEEGEEEEETEELGHAETYADYVPSKSKI	206
Q7TNB8-3	SBNO2 MOUSE	81	--EDPV--TSLSSTPLLISYQ-SH---SQPEEEEGEEEEETEELGHAETYADYVPSKSKI	132
Q9Y2G9	SBNO2 HUMAN ISO1	159	--EDFL--PS-HSTPLLVSYQ-EQSVQSQPEEEDEAEEEEAEELGHTETYADYVPSKSKI	212
Q9Y2G9-3	SBNO2 HUMAN ISO2	102	--EDFL--PS-HSTPLLVSYQ-EQSVQSQPEEEDEAEEEEAEELGHTETYADYVPSKSKI	155
A0A0G2JZZ8	SBNO2 RAT	161	-RLDEL--NAIL-SPSVAGFKAAAAPAPPPEEEEEADDEETEELGHADTYAEYKPSRSTI	216
D3ZDU8	SBNO2 RAT	155	--EDPV--TAVSSTPLLVSYQ-SH---SQPEEEEGEDEEEAEELGHAETYADYVPSKSKI	206
E7F5T6	DANRE	88	--EDPV--TAVSSTPLLVSYQ-SH---SQPEEEEGEDEEEAEELGHAETYADYVPSKSKI	139
A0A0G2KGP5	DANRE	151	-SLDDI--SAIINTPPIGGY---QRPQTQPEEEEVDVEEAAEELGHVDTYADYKPSKSKI	204
A0A2R8PYX0	DANRE	79	-SLDDI--SAIINTPPIGGY---QRPQTQPEEEEVDVEEAAEELGHVDTYADYKPSKSKI	132
A8JUV0	SBNO DROME	387	SPNQPMNPGAMVTSAAAA----AAHASAVAYVQQEEDEVDYEMGVAETYADYMPAKLKL	442
A8JUV0-3	SBNO DROME	281	SPNQPMNPGAMVTSAAAA----AAHASAVAYVQQEEDEVDYEMGVAETYADYMPAKLKL	336

Supplementary Figure 3: SBNO2 structural and phylogenetic analysis. (a) AF-Q9Y2G9-F1 alpha fold artificial intelligence-based prediction of the human SBNO2 ISO1 structure. The colour indicates the confidence of prediction. (b) Consurf-based prediction of SBNO2 phylogenetic conservation visualised on the AF-Q9Y2G9-F1 model. (c) Visualisation of SBNO2 NTP hydrolase domain (purple) and Helicase C domain (turquoise), and (d) visualisation of differences in SBNO2 ISO1 and SBNO2 ISO2 protein sequence using the AF-Q9Y2G9-F1 model. (e) Phylogenetic tree of SBNO2 isoforms across selected species. (f) Multiple sequence alignment of protein sequences of select SBNO2 isoforms according to (e). Amino acid 1 – 212 of human SBNO2 ISO1 (QY92G9) and corresponding residues of selected species are shown.

Supplementary Figure 4

Supplementary Figure 4: Analyses of ectopic SBNO2 isoform expression and localization in HEK293 cells. (a-c) Confocal microscopy images of HEK293 cells expressing Myc-tagged SBNO2 ISO1 (cyan hot) (a), HA-tagged SBNO2 ISO2 (red) (b), and co-transfected HEK293 cells expressing both SBNO2 isoforms (c). Nuclear DAPI staining and co-transfected GFP fluorescence signals are shown in sepia and green colour respectively. Source data are provided as a Source Data file for Supplementary Figures 4a-c.

Supplementary Table 1: RISK cohort patient information.

	No IBD			CD non inflamed			CD microscopic inflammation			CD macroscopic inflammation		
	Age	Sex	BMI	Age	Sex	BMI	Age	Sex	BMI	Age	Sex	BMI
Minimum	4.5		12.59	7.833		13.61	2.25		12.98	5.083		12.78
1st Quartile	10.44		16.52	10.38		14.29	10.77		16.03	10.67		14.69
Median	12.88		19.54	11.5		16.3	13.04		17.8	12.42		16.43
Mean	12.37		20.49	12.07		16.86	12.67		18.45	12.45		17.36
3rd Quartile	14.85		23.51	13.79		18.4	15.21		20.35	14.58		19.01
Maximum	18		33.24	16.58		23.75	16.92		25.27	16.83		36.46
Male		n=38			n=17			n=14			n=93	
Female		n=28			n=8			n=10			n=50	

Supplementary Figure 5
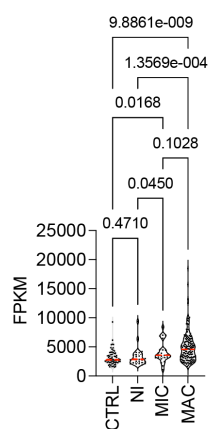
CTRL: No IBD

NI: CD not inflamed

MIC: CD microscopic inflammation

MAC: CD macroscopic inflammation
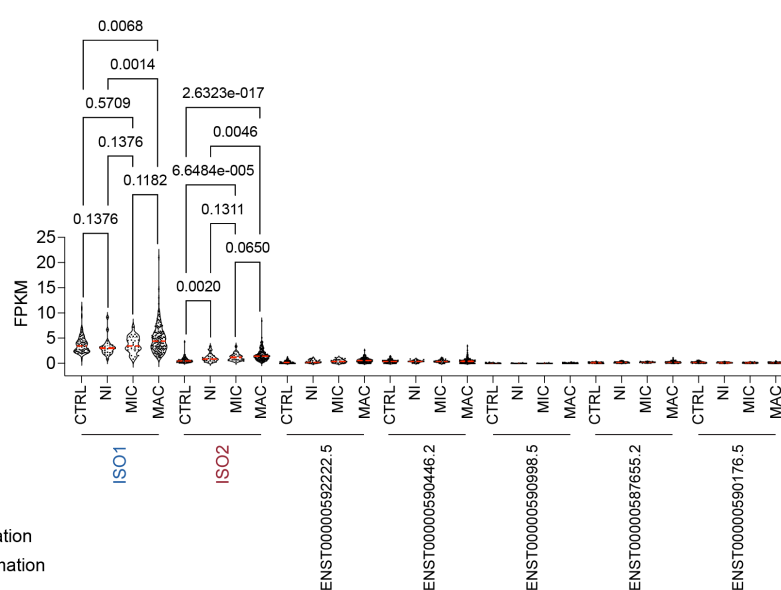
Supplementary Figure 5: *SBNO2* gene and isoform-level expression in intestinal biopsies from healthy individuals and patients with CD. (a) RNA sequencing-based estimation of *SBNO2* gene expression (non-parametric, two-sided, Kruskal-Wallis test) and (b) *SBNO2* isoforms expression in the RISK cohort data expressed as fragments per kilobase of exon per million mapped fragments (FPKM) (non-parametric, two-sided, Kruskal-Wallis test). Source data are provided as a Source Data file for Supplementary Figures 5a and b.

Supplementary Figure 6

SBNO2

Steady state
isoform (Q9Y2G9;K7ES28;Q9Y2G9–3)

Activated
isoform (Q9Y2G9;K7ES28;Q9Y2G9–3)
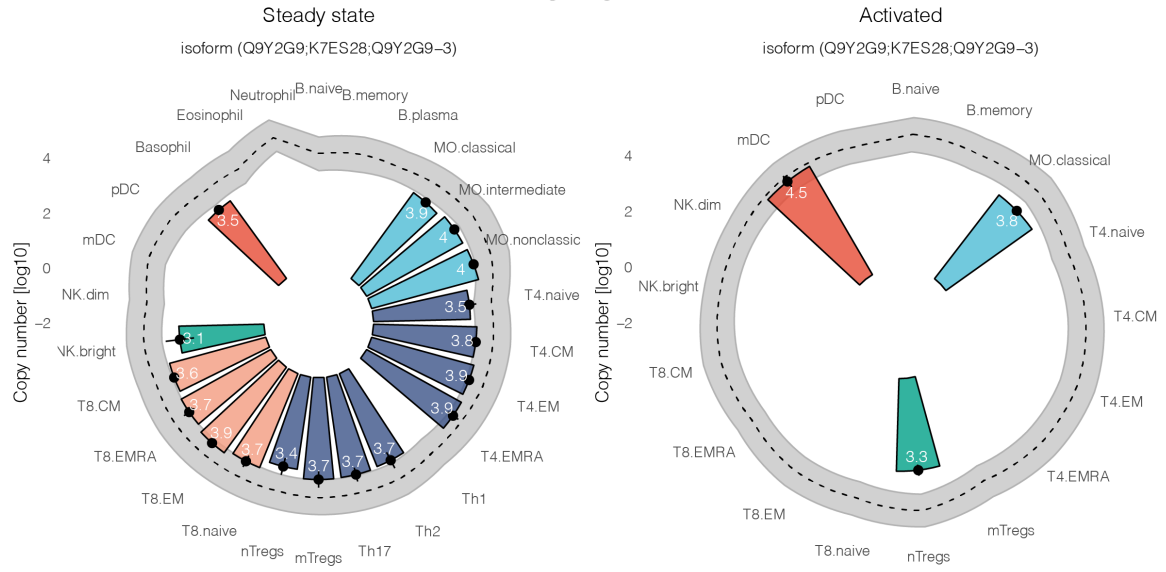
Supplementary Figure 6: Analyses of SBNO2 protein expression peripheral blood immune cells. Absolute protein copy numbers (log10) from high-sensitivity mass spectrometry quantification of SBNO2 in FACS-sorted peripheral blood immune cell types, in steady state and following stimulation (activated)[27]. The grey ribbon corresponds to the interquartile range of protein expression for all analytes in each cell.

Supplementary Figure 7

a

b

tQTL rs12973759 & SBNO2 ISO1
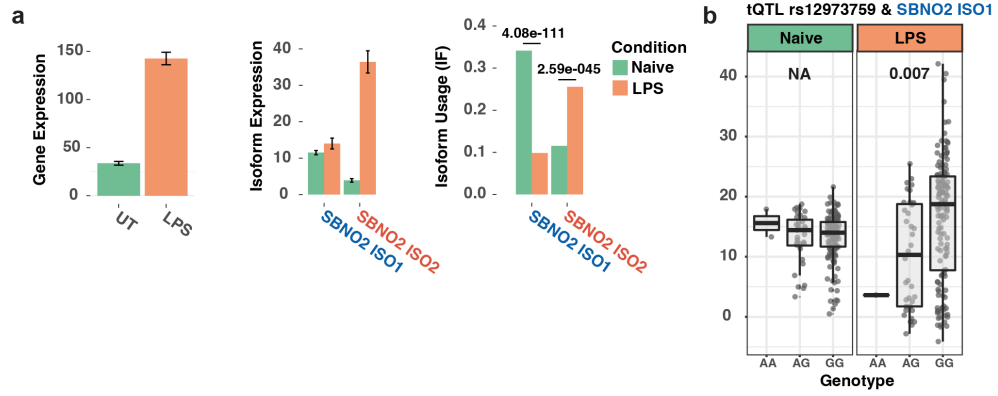
Supplementary Figure 7: *SBNO2* gene and isoform level expression in primary human monocytes. (a) *SBNO2* gene expression, *SBNO2* ISO1 and *SBNO2* ISO2 expression, and *SBNO2* ISO1 and *SBNO2* ISO2 isoform usage in resting and 24 hrs LPS-stimulated primary human monocytes (n = 176, we applied the IsoformSwitchAnalyzeR tool to analyse isoform usage in naïve and treated monocytes with LPS. Isoform usage refers to the fraction value of the mean isoform expression given the mean expression of the corresponding gene in a setting with k biological replicates). (b) Example of a variant (rs12973759) with a tQTL specifically affecting *SBNO2* ISO1 expression in LPS-stimulated CD14$^+$ monocytes. Box plots depict the interquartile range as the lower and upper bounds, respectively. The whiskers represent minimum and maximum, and the centre depicts the median. eQTL analysis was performed with the FastQTL and QTLtools using a linear regression. To allow comparison with output of the regression model the optimal number of PC was used to regress out expression changes attributable to the effect of the non-genetic covariates in local association plots. Source data are provided as a Source Data file for Supplementary Figures 7a and b.

Supplementary Table 2: Information on healthy individuals recruited via the Oxford Biobank (n = 176).

	Age	Sex	BMI
Minimum	31		17.43
1st Quartile	35		22.19
Median	49		24.29
Mean	47.22		25.19
3rd Quartile	57		26.98
Maximum	66		43.04
Male		n=60	
Female		n=116	

Supplementary Figure 8

a
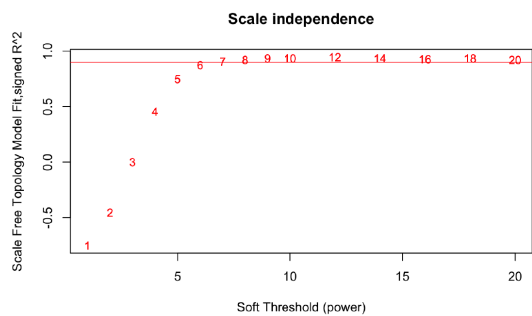
b
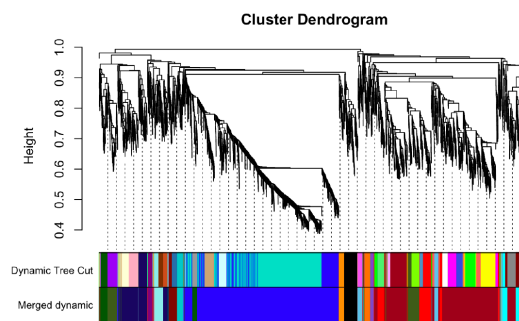
c

Supplementary Figure 8: WGCNA analysis of RNA-seq data generated from unstimulated, IL-10-, LPS, and LPS + aIL10R-stimulated MDM. (a) WGCNA soft power plot. (b) Cluster dendrogram. (c) Eigengene dendrogram including genes and transcripts of interest: *SBNO2*, *SBNO2* ISO1, and *SBNO2* ISO2.

Supplementary Table 3: Summary of MAGMA[33]-based gene-set heritability analysis.

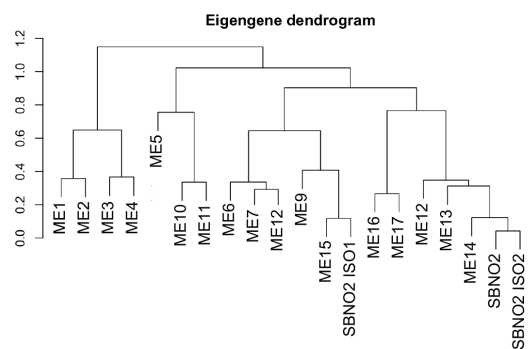| IBD							
VARIABLE	TYPE	NGENES	BETA	BETA_STD	SE	P	-LOG10(pvalue)
ME1	SET	918	0.091263	0.019998	0.031429	0.0018458	2.733815358
ME2	SET	235	0.05913	0.0066842	0.063221	0.17483	0.757384042
ME3	SET	252	0.080271	0.0093921	0.057515	0.081419	1.089274236
ME4	SET	305	-0.012925	-0.0016613	0.054697	0.5934	0.226652458
ME5	SET	53	0.23633	0.012752	0.13181	0.036496	1.437754732
ME6	SET	61	-0.0060427	-0.00034971	0.11719	0.52056	0.283529206
ME7	SET	118	-0.062614	-0.0050319	0.081982	0.77749	0.109305188
ME8	SET	50	-0.15116	-0.0079225	0.13264	0.87277	0.05910019
ME9	SET	120	0.21039	0.01705	0.089683	0.0094944	2.022532475
ME10	SET	153	0.13018	0.011902	0.077989	0.047542	1.322922552
ME11	SET	38	0.2006	0.0091689	0.14706	0.086274	1.064120066
ME12	SET	97	0.060824	0.0044344	0.094536	0.25999	0.585043356
ME13	SET	33	0.096503	0.0041109	0.18115	0.29712	0.527068114
ME14	SET	82	0.12018	0.0080594	0.11393	0.14575	0.836391437
ME15	SET	1438	0.1419	0.038324	0.026382	3.80E-08	7.419827998
ME16	SET	40	-0.041376	-0.0019401	0.14555	0.6119	0.213319547
ME17	SET	93	0.032885	0.0023478	0.095212	0.3649	0.437826137
CD							
VARIABLE	TYPE	NGENES	BETA	BETA_STD	SE	P	-LOG10(pvalue)
ME1	SET	918	0.070448	0.015439	0.030936	0.011394	1.943323785
ME2	SET	235	0.057781	0.0065328	0.062689	0.17834	0.748751238
ME3	SET	252	0.076924	0.0090019	0.055966	0.084657	1.072337126
ME4	SET	305	-0.023835	-0.003064	0.054534	0.66896	0.17459985
ME5	SET	53	0.063144	0.0034076	0.1295	0.31292	0.504566678
ME6	SET	61	-0.15992	-0.0092565	0.11426	0.91917	0.036604159
ME7	SET	118	-0.0050225	-0.0004037	0.081024	0.52471	0.280080659
ME8	SET	50	-0.01468	-0.00076951	0.13234	0.54416	0.264273385
ME9	SET	120	0.12528	0.010154	0.090237	0.082528	1.08339868
ME10	SET	153	0.076462	0.0069914	0.075688	0.1562	0.80631897
ME11	SET	38	0.1205	0.0055087	0.14354	0.2006	0.697669071
ME12	SET	97	0.18849	0.013744	0.0879	0.016008	1.795662924
ME13	SET	33	0.38933	0.016588	0.18343	0.016907	1.771933447
ME14	SET	82	0.0042318	0.00028383	0.10963	0.4846	0.31461659
ME15	SET	1438	0.09979	0.026956	0.026036	6.36E-05	4.196816111
ME16	SET	40	0.049797	0.0023354	0.15539	0.37431	0.42676857
ME17	SET	93	0.16664	0.011899	0.092567	0.035927	1.444579046
UC							
VARIABLE	TYPE	NGENES	BETA	BETA_STD	SE	P	-LOG10(pvalue)
ME1	SET	918	0.05496	0.012046	0.029513	0.031291	1.504580557
ME2	SET	235	0.0060121	0.00067979	0.058251	0.4589	0.338281942
ME3	SET	252	0.032884	0.0038485	0.052979	0.2674	0.572838597
ME4	SET	305	0.04416	0.0056773	0.052271	0.19911	0.700906928
ME5	SET	53	0.22172	0.011966	0.12522	0.038323	1.416540501
ME6	SET	61	0.039947	0.0023124	0.10657	0.35389	0.451131709
ME7	SET	118	0.031772	0.002554	0.078617	0.34306	0.464629917
ME8	SET	50	-0.15595	-0.0081757	0.12574	0.89256	0.04936258
ME9	SET	120	0.14046	0.011386	0.085852	0.050917	1.293137193
ME10	SET	153	0.10037	0.0091785	0.072839	0.084108	1.075162694
ME11	SET	38	0.14439	0.006601	0.1367	0.14544	0.837316134
ME12	SET	97	-0.11286	-0.0082303	0.087245	0.90209	0.044750131
ME13	SET	33	-0.038694	-0.0016487	0.17146	0.58927	0.229685668
ME14	SET	82	0.13138	0.0088125	0.10591	0.10741	0.968955283
ME15	SET	1438	0.078853	0.021302	0.024584	6.71E-04	3.17357531
ME16	SET	40	0.10553	0.0049498	0.1434	0.23089	0.636594876
ME17	SET	93	-0.00021387	-0.000015273	0.088658	0.50096	0.30019695

Supplementary Figure 9

	ME1	Top Module Eigengenes
Lysosome		COLGALT1, HK1, SLC8B1, IMMT, CALHM2, GPR21, SCAMP4, ARHGAP4, CTBP1, ZNF592, GDE1, HADHB
Vesicle-mediated transport		
cytoplasmic translation		
endocytosis		
Neutrophil degranulation		
translation		

-log10 P-value
40
20

ME1
COLGALT1, HK1, SLC8B1, IMMT, CALHM2, GPR21, SCAMP4, ARHGAP4, CTBP1, ZNF592, GDE1, HADHB

ME2
- regulation of autophagy
- myeloid cell apoptotic process
- apoptotic signaling pathway
- Neutrophil degranulation
- maintenance of synapse structure
- RHOH GTPase cycle

GALNT1, SLC12A6, UBXN7, WIPI2, MAPK1, ABHD4, CYHR1, EIF4EBP2, SLC38A2, IP6KI, KCTD20, PITPNM1

ME3
- Cellular responses to stimuli
- Response to metal ions
- covalent chromatin modification
- NIK-->noncanonical NF-kB signaling
- regulation of chromatin organization
- macroautophagy

MT1H, MT1F, MT1G, BAZ1B, PPP2R5D, MAP7D1, DYNLL2, MT1E, MT1X, H1-0, LAMC1, PSMD3

ME4
- Golgi vesicle transport
- PTEN Regulation
- skeletal system development
- proteolysis involved in cellular protein catabolic process
- Signal transduction by L1
- HIV Infection

SLAIN2, HIF1AN, FAF2, EDEM3, MMADHC, MARCHF6, LCP1, APLP2, CENPBD1P1, TRIM41, HDAC1, ARSD

ME5
- Thyroid hormone synthesis
- lipid storage
- cellular monovalent inorganic cation homeostasis
- negative regulation of leukocyte differentiation
- regulation of response to endoplasmic reticulum stress
- glycerophospholipid biosynthetic process

PAX8-AS1, ERP29, TRABD, SLFN11, ANP32A, WASHC2A, TMEM109, TOR3A, GSTK1, SCAMP3, PLEC, MGA

ME6
- mRNA processing
- mRNA surveillance pathway
- peptidyl-lysine modification
- mRNA polyadenylation
- Intra-Golgi and retrograde Golgi-to-ER traffic
- cellular response to glucose stimulus

LSM14A, PPID, GCC1, IWS1, CASC3, R3HDM4, MFAP1, TM9SF4, MRPL28, MAP3K11, TFIP11, YTHDC1

ME7
- Deactivation of the beta-catenin transactivating complex
- N-glycan trimming in the ER and Calnexin/Calreticulin cycle
- proteasomal protein catabolic process
- Hh mutants are degraded by ERAD
- alpha-Linolenic acid metabolism
- negative regulation of DNA-templated transcription, elongation

EMC7, AFTPH, PEF1, H2AC19, TMBIM4, TMEM167B, NFE2L1, QSOX1, ACTN4, MT2A, HEXIM1, DCAF5

ME8
- Deactivation of the beta-catenin transactivating complex
- Protein processing in endoplasmic reticulum
- regulation of protein-containing complex disassembly
- positive regulation of inflammatory response
- regulation of proteolysis involved in cellular protein catabolic process
- Spliceosome

PTPA, GNPTAB, CES1, ENTPD1, SIL1, C1QA, ADAMDEC1, ATP6AP1, CTSC, C6orf47, ARPC5, OSCAR

ME9
- Staphylococcus aureus infection
- positive regulation of immune response
- Neutrophil degranulation
- Complement cascade
- regulation of CD4-positive, CD25-positive, alpha-beta regulatory T cell differentiation
- oxidative phosphorylation

CTSS, CNDP2, ABCD1, FGD2, HLA-DRB1, C1QB, LAMP2, HLA-DRA, SERPING1, LGALS9, ACTG1, HLA-DPA1

ME10
- L13a-mediated translational silencing of Ceruloplasmin expression
- Translation initiation complex formation
- ribonucleoprotein complex biogenesis
- ribosomal large subunit biogenesis
- regulation of translation
- mitochondrial transmembrane transport

SLC52A2, RPL18A, RPS15, RPL10A, EIF4A1, ABCG1, RPS5, RPS8, RPL5, GUSB, RPL14, RPL12

ME11
- Lysosome
- lysosome organization
- regulation of cell-cell adhesion
- Formation of the ternary complex, and subsequently, the 43S complex
- receptor metabolic process
- Antigen processing and presentation

CD4, IFI30, CD81, HSP90AB1, EIF3C, TSPAN4, NAGLU, GNPTG, HLA-DMA, CFD, LYZ, LRPAP1

ME12
- Macroautophagy
- Ubiquitin mediated proteolysis
- Autophagy - animal
- Signaling by Receptor Tyrosine Kinases
- cellular monovalent inorganic cation homeostasis
- endoplasmic reticulum to Golgi vesicle-mediated transport

NAV1, FCHSD2, CARM1, HSBP1, BNIP3L, PTGES3, TNFRSF1A, EIF3D, XRCC5, CAP1, PCBP2, HSPB1

ME13
- cellular pigmentation
- negative regulation of mitotic cell cycle
- Adaptive Immune System
- Hemostasis
- regulation of cell development
- positive regulation of myoblast fusion

PNKD, BCL6, KIF3C, LIAR1, TLR1, DCTN2, NIBAN2, CTDSP2, PLIN3, PHC2, H3-3A, EFHD2

ME14
- Jak-STAT signaling pathway
- sulfur compound biosynthetic process
- Acute myeloid leukemia
- RHOB GTPase cycle
- cellular response to interleukin-6
- Cytokine Signaling in Immune system

DSE, SLC2A3, STAT3, SOCS3, CD53, **SBNO2**, BACH1, PTPN2, PPP1CB, APIP, HNRNPH2, UBE2J1

ME15
- Interferon Signaling
- Class I MHC mediated antigen processing & presentation
- viral process
- Cellular responses to stress
- cytokine-mediated signaling pathway
- regulation of actin cytoskeleton organization

SETD5, CYLD, CDC42SE1, N4BP1, BAZ2A, B4GALT1, E2F3, DESI1, MSC, C15orf48, SRC, COPG1

ME16
- regulation of actin cytoskeleton organization
- positive regulation of focal adhesion assembly
- Pathogenic Escherichia coli infection
- regulation of mRNA metabolic process
- regulation of intrinsic apoptotic signaling pathway
- muscle cell migration

RBM3, CGGBP1, SFPQ, FASTK, MFSD10, ABCA1, SLC35F5, TMBIM6, ACBD5, ARFGAP1, TPT1, DIDO1

ME17
- ubiquitin-dependent protein catabolic process
- dosage compensation by inactivation of X chromosome
- regulation of cell growth involved in cardiac muscle cell development
- nuclear-transcribed mRNA catabolic process, deadenylation-dependent decay
- generation of precursor metabolites and energy
- Maturation of nucleoprotein

CTDP1, MON1B, UBE2J2, PIGG, DLST, ILF2, NIPA2, AREL1, NR2C2, MYO1C, EIF3I, KCNN4
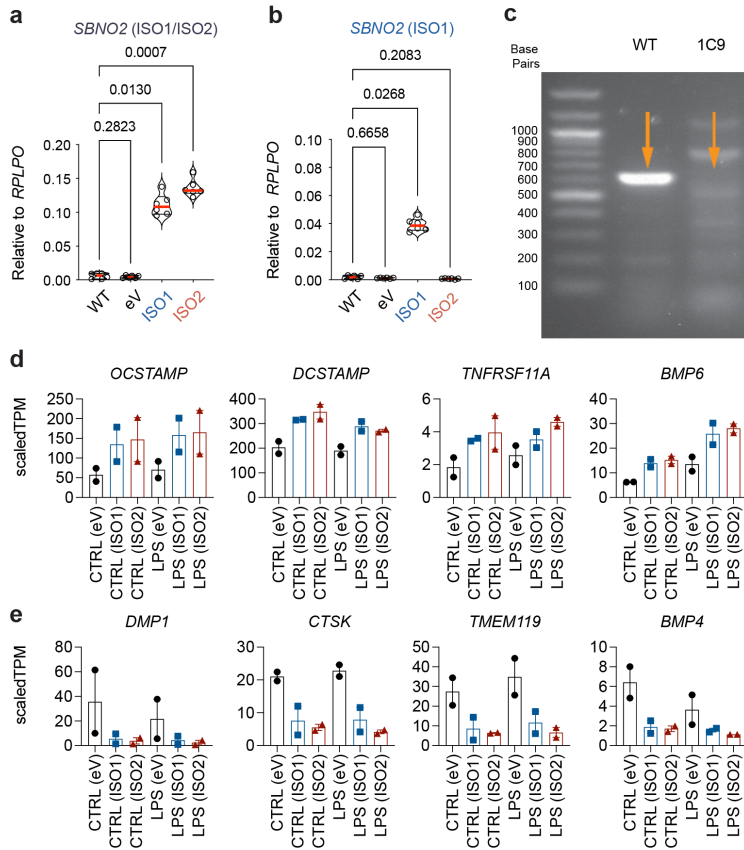
Supplementary Figure 9: Pathway analysis of WGCNA gene modules identified in unstimulated, IL-10-, LPS, and LPS + aIL10R-stimulated MDM. Metascape enrichment of KEGG, Reactome, and GO pathway terms based on those gene modules that were identified in unstimulated MDM and 8 hrs IL-10 (100 ng/mL), LPS (200 ng/mL), or LPS + aIL-10R (200 ng/mL, 10 µg/mL) stimulated MDM (hypergeometric test, Bonferroni correction, padj<0.05). Genes listed on the right represent the respective top 12 correlated module eigengenes. Source data are provided as a Source Data file for Supplementary Figure 9.

Supplementary Figure 10

a *SBNO2 (ISO1)*

b *SBNO2 (ISO1)*

SBNO2 (ISO1/ISO2)

SBNO2 (ISO1/ISO2)

c Increased expression - Negative regulation

d Decreased expression - Positive regulation

e

CTRL — hsa04380 (TOP5/5): ITGB3, RELB, SOCS3, ACP5, NFKB2, FCGR1A, AKT3, CSFR1, NCF4, TGFBR2

Cell surface interactions at the vascular wall; Cell adhesion molecules; Phagosome; Regulation of smooth muscle cell proliferation; Positive regulation of epithelial cell migration; Positive regulation of cell-cell adhesion; Myeloid cell differentiation; MAPK signaling pathway; C-type lectin receptor signaling pathway; Osteoclast differentiation

LPS — hsa04060 (TOP5/5): IL20, ACKR3, CSF2, IL23A, IL24, CCL1, CXCL9, CSFR1, CXCL10, TNFRSF

Cytokine-cytokine receptor interaction; Cell chemotaxis; Phagocytosis; Interleukin-4 and Interleukin-13 signaling; Viral protein interaction with cytokine and cytokine receptor; Rheumatoid arthritis; Cellular response to molecule of bacterial origin; JAK-STAT signaling pathway; Interleukin-10 signaling

IL-10 — GO:0022409 (TOP5/5): CD70, CCR7, ADA, TNFSF9, PPAP2B, IGFBP2, IL7, IL2RA, SOCS1, ETS1

Positive regulation of cell-cell adhesion; Positive regulation of inflammatory response; G alpha (i) signalling events; Leukocyte chemotaxis; Positive regulation of leukocyte cell-cell adhesion; GPCR ligand binding; Interleukin-4 and Interleukin-13 signaling; Cytokine-cytokine receptor interaction; Phagosome; Class A/1 (Rhodopsin-like receptors)

LPS + aIL-10R — GO:0070372 (TOP5/5): DUSP4, CCL22, LIF, FN1, GPR183, GBP1, SPRY4, CCL15, CSFR1, CCL1

Cytokine-cytokine receptor interaction; Leukocyte chemotaxis; Myeloid leukocyte migration; Regulation of erk1 and erk2 cascade; Platelet activation, signaling and aggregation; Cellular response to molecule of bacterial origin; Rheumatoid arthritis; Angiogenesis; Viral entry into host cell; Interleukin-4 and Interleukin-13 signaling

Supplementary Figure 10: siRNA-mediated knockdown of SBNO2 in primary human MDM. (a and b) RT-qPCR analysis of *SBNO2* ISO1 (a) and *SBNO2* ISO1/ISO2 (b) expression in primary human MDM shown as relative expression to *RPLPO* (left) and fold change to control siRNA-treated MDM (right) (Independent experiments/donors: n = 6/13; nonn-parametric, two-sided, Friedman test). (c and d) Venn diagrams show the numbers of significantly ($\log_2$ fold change > 0.25, padj<0.05, FDR) differentially up-regulated (c) and down-regulated (d) genes upon knockdown of *SBNO2* in MDM (n=3) comparing unstimulated (CTRL), IL-10- (100 ng/mL), LPS- (200 ng/mL), or LPS+aIL-10R-treated (200 ng/mL, 10 µg/mL) conditions by RNA-seq and DESeq2 (n=3). (e) STRING functional enrichment analysis showing the top 10 enriched pathways (GO Biologic Process, KEGG Pathways, Reactome Pathways) with dual distribution based on DESeq2 differential expression ranking and functional enrichment analysis false discovery rate. Each one selected pathway is highlighted. The respective top 5 SBNO2 knockdown upregulated and top 5 SBNO2 knockdown downregulated (FDR) pathway genes are listed and the distribution according to $\log_2$ fold change expression across the dataset visualized. Source data are provided as a Source Data file for Supplementary Figures 10a and b.

Supplementary Figure 11

a *SBNO2* (ISO1/ISO2)

b *SBNO2* (ISO1)

c

d

e

Supplementary Figure 11: Ectopic expression and CRISPR-Cas9-mediated knockout of SBNO2 in the THP-1 cell line. (a and b) RT-qPCR analysis of (a) *SBNO2* ISO1/ISO2, and (b) *SBNO2* ISO1 expression in lentivirus transduced, GFP⁺-sorted, and PMA-differentiated THP-1 MDM (Independent experiments/replicates: n = 2/6, non-parametric, two-sided, Kruskal-Wallis test). (c) Agarose gel image showing the results from a PCR amplification of genomic DNA of the CRSPR-Cas9-targeted *SBNO2* region in WT THP-1 monocytes and a THP-1 single cell clone (1C9). (d) Expression of *OCSTAMP*, *DCSTAMP*, *TNFRSF11A*, and *BMP6* in lentivirus-transduced (empty vector (eV), SBNO2 ISO1 (ISO1), and SBNO2 ISO2 (ISO2)) THP-1 MDM in steady state or following 8 hrs stimulation with 200 ng/mL LPS measured by RNA-seq (n = 2). (e) Expression of *DMP1*, *CTSK*, *TMEM119*, and *BMP4* according to (d) (n = 2). Source data are provided as a Source Data file for Supplementary Figures 11a-e.